

$\chi_{cJ} \rightarrow e^+e^-$ decays revisited

N. Kivel¹ and M. Vanderhaeghen

*Helmholtz Institut Mainz, Johannes Gutenberg-Universität,
D-55099 Mainz, Germany*

*Institut für Kernphysik, Johannes Gutenberg-Universität,
D-55099 Mainz, Germany*

E-mail: kivel@kph.uni-mainz.de, marcvdh@kph.uni-mainz.de

ABSTRACT: We present a calculation of the width for $\chi_{cJ} \rightarrow e^+e^-$ decay. The amplitude of the process is computed within the NRQCD framework. The leading-order contribution is described by two terms associated with the two different integration domains in the electromagnetic loop describing two-photon annihilation of the heavy quark-antiquark pair. The corresponding operators are defined in the framework of NRQCD. The matrix element of one of these operators describes a configuration with an ultrasoft photon and can be associated with the higher Fock state of the heavy meson. In order to compute this contribution we use the heavy hadron chiral perturbation theory. We obtain that this contribution is numerically dominant. The obtained estimates for the decay widths of the χ_{c1} and χ_{c2} states are 0.09 eV and 0.07 eV, respectively.

KEYWORDS: e+e- Experiments, Charm physics

ARXIV EPRINT: [1509.07375](https://arxiv.org/abs/1509.07375)

¹On leave of absence from St. Petersburg Nuclear Physics Institute, 188350, Gatchina, Russia.

Contents

| | | |
|----------|--|-----------|
| 1 | Introduction | 1 |
| 2 | Kinematics and notation | 2 |
| 3 | Factorization of decay amplitudes in NRQCD | 5 |
| 4 | Phenomenology | 14 |
| 4.1 | Calculation of the ultrasoft matrix element in the heavy hadron chiral perturbation theory | 14 |
| 4.2 | Numerical estimates | 16 |
| 5 | Conclusions | 19 |

1 Introduction

The leptonic decays of C-even charmonium states into a lepton pair have a very small branching ratio because they can only occur via a two-photon intermediate state $\chi_{cJ} \rightarrow \gamma^* \gamma^* \rightarrow e^+ e^-$. However with the high-luminosity BEPC-II $e^+ e^-$ -accelerator operating on the charmonium energy region such measurements of direct production cross section $e^+ e^- \rightarrow \chi_{cJ}$ become feasible. The study of the mechanism of the production of C-even quarkonium states is especially interesting in view of the production of higher resonances such as the exotic charmonium-like state X(3872).

The decays $\chi_{cJ} \rightarrow l^+ l^-$ have already been studied long time ago in ref. [1]. The authors considered the quarkonium description and a vector dominance model (VDM) in order to describe the decay amplitudes of charmonium states with $J = 1, 2$. It was found that a naive quarkonium description is problematic because of infrared logarithmic divergencies arising in the integrals describing the quark-photon annihilation loop. Such divergencies indicate that the corresponding contribution is also sensitive to long distance physics. The corresponding integrals in ref. [1] have been regularized by introducing the binding energy $M_\chi - 2m_Q \simeq 500$ MeV. The numerical estimates obtained in this way give very small value of the widths, smaller than bounds derived from analyticity and unitarity in the same work. Probably, a more realistic estimate was obtained using generalized VDM which yields a larger numerical value for the widths, consistent with the unitarity constrains: $\Gamma[\chi_{c1} \rightarrow e^+ e^-] \simeq 0.46$ eV and $\Gamma[\chi_{c2} \rightarrow e^+ e^-] \simeq 0.014$ eV [1].

Recently the decay rate of the χ_{c1} state was again estimated in [2] using the VDM approach, with result $\Gamma[\chi_{c1} \rightarrow e^+ e^-] \simeq 0.1$ eV. The short distance contributions describing a configuration with highly virtual photons were considered in this framework as unknown contact vertices giving rise to a theoretical uncertainty.

The aim of the present work is to provide a more systematic description of the decay amplitudes for $\chi_{cJ} \rightarrow \gamma^* \gamma^* \rightarrow e^+ e^-$ process using the NRQCD factorization framework [4, 5], see also review [6] and references therein. This technique allows one to perform a systematic description of heavy quarkonium states using the small relative velocity of heavy quarks and the small QCD running coupling at short distances. Within this framework we associate the IR-divergencies found in [1] with a specific quark-photon operator which describes a configuration with an ultrasoft photon. The matrix element of this operator describes the overlapping with the higher Fock state which consists of heavy quark-antiquark and photon. This allows us to perform a systematic separation and description of the different contributions relevant in a leading-order expansion in small velocity v .

Our paper is organized as follows. In section 2 we briefly describe our notation and provide definitions of various quantities used in the following. Section 3 is devoted to the investigation of the one-loop integral which describes the leading-order contribution. In this section we establish the dominant regions and provide a description of the amplitude within the NRQCD factorization framework. Section 4 is devoted to the calculation of the ultrasoft photon matrix element in the heavy hadron chiral effective theory (HH χ PT). Furthermore, a estimate of the decay rates is given. In section 5 we briefly summarize our results.

2 Kinematics and notation

Let us start from the description of the decay kinematics $\chi_{cJ}(P) \rightarrow e^+(l_1)e^-(l_2)$. The initial state momentum can be written as

$$P = M_\chi \omega, \quad \omega^2 = 1, \tag{2.1}$$

where ω denotes the charmonium velocity. In the following, we consider the charmonium rest frame which implies

$$\omega = (1, \vec{0}). \tag{2.2}$$

The small relative velocity of heavy quarks in the bound state is denoted as v . Neglecting lepton masses, the lepton momenta can be written as

$$l_1 = M_\chi \frac{n}{2}, \quad l_2 = M_\chi \frac{\bar{n}}{2}, \tag{2.3}$$

where n and \bar{n} denote the light-like vectors which satisfy $(n \cdot \bar{n}) = 2$. Any 4-vector V^μ can be expanded as

$$V^\mu = (V \cdot n) \frac{\bar{n}^\mu}{2} + (V \cdot \bar{n}) \frac{n^\mu}{2} + V_\perp^\mu, \tag{2.4}$$

where V_\perp denotes the components transverse to the light-like vectors: $(V_\perp \cdot n) = (V_\perp \cdot \bar{n}) = 0$. Similarly, one can also write a decomposition

$$V^\mu = (V \cdot \omega) \omega^\mu + V_\top^\mu, \tag{2.5}$$

where V_\top denotes the component which is orthogonal to the velocity ω : $(\omega \cdot V_\top) = 0$. In the following we assume that in the rest frame

$$\omega = \frac{n}{2} + \frac{\bar{n}}{2}. \tag{2.6}$$

The momenta of the heavy quark and antiquark with mass m which form a quarkonium state can be written as

$$p_1 = \frac{1}{2}P + \Delta, \quad p_2 = \frac{1}{2}P - \Delta, \quad (2.7)$$

where the relative momentum Δ satisfies

$$(\Delta \cdot \omega) = 0, \quad \Delta^2 = -\vec{\Delta}^2. \quad (2.8)$$

The heavy quarks which create a bound state are non-relativistic, implying that the relative velocity $v \sim \Delta/m$ is quite small: $v \ll 1$.

The power counting rules of NRQCD has been established in [3, 4]. Following these arguments we assume that the mass m is large enough and that the most important scales such as mass m , typical three-momentum of the heavy quark $\sim mv$ and its typical kinetic energy $\sim mv^2$ satisfy

$$(mv^2)^2 \ll (mv)^2 \ll m^2. \quad (2.9)$$

Integrating out the modes with hard momenta $p_h \sim m_c$ one passes onto the effective theory NRQCD which describes the modes with the soft momenta $p_s \sim mv$. If the scale $mv \gg \Lambda_{QCD}$ then one can integrate over the soft region together with potential gluons with momenta [5, 7–10]

$$p_0 \sim mv^2, \quad \vec{p} \sim m\vec{v}, \quad (2.10)$$

After this one obtains a new effective theory which is known as potential NRQCD (pNRQCD). For a more detailed information about these effective theories see ref. [6] and references therein.

The charm quark mass $m_c \simeq 1.5 \text{ GeV}$ is not large enough compared to Λ_{QCD} therefore in this case one can only factorize the effects at momentum scales of order m_c . However, in the QED sector one can also consider the possibility to integrate over the soft region too. As we will show further on, such situation is relevant for the factorization of the electromagnetic loop describing the transition $c\bar{c} \rightarrow \gamma^* \gamma^* \rightarrow e^+ e^-$.

After factorization of the hard contribution, the nonperturbative QCD dynamics is described by the matrix elements of appropriate operators defined in an effective theory. In the following, we will need the following set of NRQCD operators which describe the matrix elements between the charmonium and the vacuum states:

$$\mathcal{O}^\sigma(^3S_1) = \chi_\omega^\dagger \gamma_\top^\sigma \psi_\omega, \quad (2.11)$$

$$\mathcal{O}(^3P_0) = -\frac{1}{\sqrt{3}} \chi_\omega^\dagger \left(\frac{-i}{2} \right) \overleftrightarrow{D}_\top^\alpha \gamma_\top^\alpha \psi_\omega, \quad (2.12)$$

$$\mathcal{O}^\beta(^3P_1) = \frac{1}{2\sqrt{2}} \chi_\omega^\dagger \overleftrightarrow{D}_\top^\alpha \left(\frac{-i}{2} \right) [\gamma_\top^\alpha, \gamma_\top^\beta] \gamma_5 \psi_\omega, \quad (2.13)$$

$$\mathcal{O}^{\alpha\beta}(^3P_2) = \chi_\omega^\dagger \left(\frac{-i}{2} \right) \overleftrightarrow{D}_\top^{(\alpha} \gamma_\top^{\beta)} \psi_\omega, \quad (2.14)$$

where the covariant derivative $iD_\mu = i\partial_\mu + gA_\mu$, $\overleftrightarrow{D}_\top = \overrightarrow{D}_\top - \overleftarrow{D}_\top$. Furthermore, we use the covariant four-component fields ψ_ω, χ_ω to describe the soft quark and antiquarks

within the NRQCD framework. These fields satisfy

$$\chi_\omega^\dagger \psi = -\chi_\omega^\dagger, \quad \psi \psi_\omega = \psi_\omega. \quad (2.15)$$

Using eq. (2.2), one can show that the operators in eqs. (2.11)–(2.14) can be reduced to the set of well-known non-relativistic operators constructed from two-component Pauli spinors.

The matrix elements of these operators are well known in the literature and can be written as

$$\langle 0 | \psi_\omega^\dagger \gamma_\mp^\sigma \chi_\omega | J/\psi \rangle = \epsilon_\psi^\sigma \langle \mathcal{O}(^3S_1) \rangle, \quad (2.16)$$

$$\langle 0 | \psi_\omega^\dagger \gamma_\mp^\sigma \chi_\omega | \psi' \rangle = \epsilon_{\psi'}^\sigma \langle \mathcal{O}'(^3S_1) \rangle, \quad (2.17)$$

$$\langle 0 | \mathcal{O}(^3P_0) | \chi_{c0} \rangle = i \langle \mathcal{O}(^3P_0) \rangle, \quad (2.18)$$

$$\langle 0 | \mathcal{O}^\sigma(^3P_1) | \chi_{c1} \rangle = i \epsilon_X^\sigma \langle \mathcal{O}(^3P_0) \rangle, \quad (2.19)$$

$$\langle 0 | \mathcal{O}^{\alpha\beta}(^3P_2) | \chi_{c2} \rangle = i \epsilon_X^{\alpha\beta} \langle \mathcal{O}(^3P_0) \rangle. \quad (2.20)$$

The constants $\langle \mathcal{O}(^3S_1) \rangle$ and $\langle \mathcal{O}(^3P_0) \rangle$ are related to the value of the charmonium wave functions at the origin

$$\langle \mathcal{O}(^3S_1) \rangle = \sqrt{2N_c} \sqrt{2M_\psi} \sqrt{\frac{1}{4\pi}} R_{10}(0), \quad (2.21)$$

$$\langle \mathcal{O}'(^3S_1) \rangle = \sqrt{2N_c} \sqrt{2M_{\psi'}} \sqrt{\frac{1}{4\pi}} R_{20}(0), \quad (2.22)$$

$$\langle \mathcal{O}(^3P_0) \rangle = \sqrt{2N_c} \sqrt{2M_{\chi_{c0}}} \sqrt{\frac{3}{4\pi}} R'_{21}(0), \quad (2.23)$$

where $R_{nl}(r)$ is the radial part of the Schrödinger wave function and $R'_{nl}(r)$ denotes its derivative. The r.h.s. of eqs. (2.18)–(2.20) depends on of the same constant $\langle \mathcal{O}(^3P_0) \rangle$ due to the spin symmetry of the leading non-relativistic action [4]. The polarization vectors $\epsilon_\psi^\sigma(\lambda)$, $\epsilon_X^\beta(\lambda)$ and $\epsilon_X^{\alpha\beta}(\lambda)$ correspond to spin-1 and spin-2 charmonium states, respectively. They are normalized to satisfy

$$\sum_\lambda \epsilon_X^\sigma(\lambda) \{ \epsilon_X^\rho(\lambda) \}^* = -g^{\sigma\rho} + \frac{P^\sigma P^\rho}{M_X^2}, \quad (2.24)$$

with $X = \{ J/\psi, \chi_{c1} \}$ and

$$\sum_\lambda \epsilon_X^{\alpha\beta}(\lambda) \{ \epsilon_X^{\alpha'\beta'}(\lambda) \}^* = \frac{1}{2} M_{\alpha\alpha'} M_{\beta\beta'} + \frac{1}{2} M_{\alpha\beta'} M_{\beta\alpha'} - \frac{1}{3} M_{\alpha\beta} M_{\alpha'\beta'}, \quad (2.25)$$

with $M_{\alpha\beta} = -g_{\alpha\beta} + P_\alpha P_\beta / M_{\chi_{c2}}^2$.

The decay amplitudes $\chi_{cJ} \rightarrow e^+ e^-$ are defined as

$$\langle e^+ e^-; out | in; \chi_{cJ} \rangle = i(2\pi)^4 \delta(l_1 + l_2 - P) \mathcal{A}_J, \quad (2.26)$$

with

$$\mathcal{A}_J = \bar{u}_n \Gamma_J v_{\bar{n}} T_J, \quad (2.27)$$

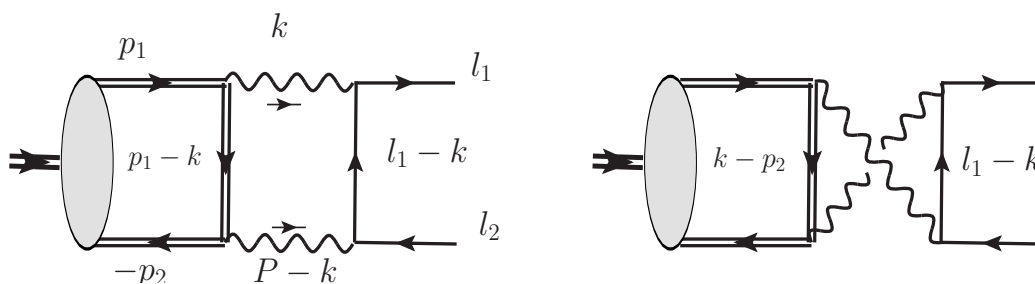


Figure 1. One-loop diagrams describing the annihilation of χ_{cJ} into an e^+e^- pair.

and where \bar{u}_n and $\bar{v}_{\bar{n}}$ denotes the spinors of the masses lepton and antilepton, respectively

$$\bar{u}_n = \bar{u}(l_1) \frac{\not{p}_1 \not{p}_2}{4}, \quad v_{\bar{n}} = \frac{\not{p}_1 \not{p}_2}{4} v(l_2), \quad (2.28)$$

and

$$\Gamma_1 = \epsilon_{\chi}^{\sigma} \gamma_{\perp\sigma} \gamma_5, \quad \Gamma_2 = \epsilon_{\chi}^{\sigma\rho} n_{\rho} \gamma_{\perp\sigma}. \quad (2.29)$$

The leading-order contribution to these amplitudes arises from the annihilation of heavy quarks into two photons which create the outgoing lepton pair, see figure 1. If the one-loop integral is dominated by the hard region where both photons and heavy quark are highly off-shell then one can expect that such process can be described within the NRQCD approach and the amplitude can be factorized into hard and soft parts. In the next section we consider this possibility in more detail.

3 Factorization of decay amplitudes in NRQCD

The leading-order in α_s diagrams describing the e^+e^- decay of C -even charmonia are shown in figure 1. These one-loop diagrams are constructed from the photon, lepton and heavy quark (double lines). The diagrams in figure 1 can be computed in the heavy quark mass limit $m \rightarrow \infty$, performing an expansion in the small parameter $\Delta/m \sim v$. Let us to start from a naive guess that the dominant contribution is only provided by the hard region where the loop momentum $k_{\mu} \sim m$, and therefore all propagators are far of off-shell. The leading-order contribution in $1/m$ is provided by projections onto the leading-order operators $\mathcal{O}({}^3P_J)$ described in eqs. (2.18)–(2.20). The technical details are well known in the literature, see e.g. [1]. The resulting expressions can be presented as

$$\mathcal{A}_1 = \epsilon_{\chi}^{\nu} i \langle \mathcal{O}({}^3P_0) \rangle e^2 \sqrt{2} \int dk \frac{\bar{u}_n \gamma_{\alpha} (\not{l}_1 - \not{k}) \gamma_{\beta} v_{\bar{n}}}{[(k - l_1)^2] [k^2] [(k - P)^2]} \frac{1}{4} \text{Tr} \left[\mathcal{P}_{1\mu\nu} \Gamma^{\alpha\beta\mu}(k) \right], \quad (3.1)$$

$$\mathcal{A}_2 = \epsilon_{\chi\mu\nu} i \langle \mathcal{O}({}^3P_0) \rangle e^2 \int dk \frac{\bar{u}_n \gamma_{\alpha} (\not{l}_1 - \not{k}) \gamma_{\beta} v_{\bar{n}}}{[(k - l_1)^2] [k^2] [(k - P)^2]} \frac{1}{4} \text{Tr} \left[\mathcal{P}_2^{\nu} \Gamma^{\alpha\beta\mu}(k) \right], \quad (3.2)$$

where the square brackets for the propagators denote the standard Feynman prescription $[A]^{-1} \equiv [A + i\varepsilon]^{-1}$. The corresponding contribution to the amplitude $\chi_{c0} \rightarrow e^+e^-$ vanishes and therefore is suppressed by a power of v and will not be considered it in this work.

The total structure of the integrands in expressions (3.1) and (3.2) can be divided into the lepton and heavy quark parts. The lepton part has $\bar{u}_n \dots v_{\bar{n}}$ in the numerator and includes the photon and lepton propagators in the denominators. The heavy quark part is given by $\text{Tr}[\mathcal{P}_i \Gamma^{\alpha\beta\mu}(k)]$. We introduced the projections \mathcal{P}_J onto charmonium states

$$\mathcal{P}_1^{\mu\nu} = \frac{1}{4}(1 + \psi)(\gamma_{\top}^{\mu}\gamma_{\top}^{\nu} - \gamma_{\top}^{\nu}\gamma_{\top}^{\mu})\gamma_5, \quad (3.3)$$

$$\mathcal{P}_2^{\nu} = (1 + \psi)\gamma_{\top}^{\nu}. \quad (3.4)$$

The expression for $\Gamma^{\alpha\beta\mu}(k)$ reads

$$\Gamma^{\alpha\beta\mu}(k) = \frac{1}{2m} \left\{ \gamma^{\mu} \hat{D}_Q(k) + \hat{D}_Q(k) \gamma^{\mu} \right\} + \hat{D}'_Q{}^{\mu}(k), \quad (3.5)$$

with

$$\hat{D}_Q = \frac{i(ie_Q)^2}{\left[k^2 - 2m(k\omega) - \vec{\Delta}^2 \right]} \left\{ \gamma^{\beta}(m\psi - \not{k} + m)\gamma^{\alpha} + \gamma^{\alpha}(\not{k} - m\psi + m)\gamma^{\beta} \right\}, \quad (3.6)$$

$$\begin{aligned} \hat{D}'_Q{}^{\mu} &= \frac{i(ie_Q)^2}{\left[k^2 - 2m(k\omega) - \vec{\Delta}^2 \right]} \left\{ \gamma^{\beta}\gamma^{\mu}\gamma^{\alpha} + \gamma^{\alpha}\gamma^{\mu}\gamma^{\beta} \right\} \\ &+ \frac{i(ie_Q)^2 2k^{\mu}}{\left[k^2 - 2m(k\omega) - \vec{\Delta}^2 \right]^2} \left\{ \gamma^{\beta}(m\psi - \not{k} + m)\gamma^{\alpha} - \gamma^{\alpha}(\not{k} - m\psi + m)\gamma^{\beta} \right\}, \end{aligned} \quad (3.7)$$

where e_Q is the charge of the heavy quark ($e_c = 2/3$). The small squared relative momentum $\vec{\Delta}^2 \sim (mv)^2$ which appears in the heavy quark propagator provides an IR-regularization and can be neglected if it is not required. With this regularization the traces and loop integrals are computed in four dimensions with $dk \equiv d^4k/(2\pi)^4$.

The expressions (3.1) and (3.2) have been obtained by expanding the heavy quark fields in position space

$$c(y) \simeq e^{-im(\omega y)} \left[1 + y \cdot \partial + \frac{1}{2m} i \not{D}_{\top} \right] \psi_{\omega}(0) \quad (3.8)$$

and projecting the soft quark fields χ_{ω}^{\dagger} and ψ_{ω} onto leading-order operators (2.12)–(2.14). The terms $\sim y \cdot \partial \psi_{\omega}$ (arising from the multipole expansion of the soft quark field arguments) lead to the expansion of the integrand with respect to small relative momentum Δ giving the contribution $D'_Q{}^{\mu}$. The terms proportional to $\sim \frac{1}{2m} \not{D}_{\top}$ give the contribution with \hat{D}_Q . The evaluation of the integrals in eqs. (3.1) and (3.2) gives

$$\mathcal{A}_1 = \bar{u}_n \Gamma_1 v_n i \langle \mathcal{O}({}^3P_0) \rangle \frac{\alpha^2}{m^3} e_Q^2 2\sqrt{2} \ln \frac{m^2}{2\vec{\Delta}^2}, \quad (3.9)$$

$$\mathcal{A}_2 = \bar{u}_n \Gamma_2 v_n i \langle \mathcal{O}({}^3P_0) \rangle \frac{\alpha^2}{m^3} e_Q^2 \left(2 \ln \vec{\Delta}^2/m^2 + \frac{2}{3} (\ln 2 - 1 + i\pi) \right). \quad (3.10)$$

These expressions are in agreement with the results obtained in ref. [1]. We obtain that both amplitudes depend on the large logarithm $\sim \ln \vec{\Delta}^2/m^2$ which is sensitive to the soft

scale $\vec{\Delta}^2$. This shows that the starting assumption about one dominant region $k \sim m$ is incorrect. There must be at least one more domain where some propagators in the loop integral are soft. One can expect that the additional region is associated with the configuration when one of the photons is soft. In this case the propagator of the heavy quark is also soft and the hard configuration is described by the tree level subdiagram describing the annihilation $c\bar{c} \rightarrow e^+e^-$ through one photon.

In order to get an idea about the explicit definition of this region it is useful to investigate the integrals of diagrams in figure 1 within the threshold expansion technique worked out in ref. [5]. According to this analysis the threshold kinematics is described by the following regions

$$\text{hard :} \quad k_\mu \sim m, \tag{3.11}$$

$$\text{soft :} \quad k_\mu \sim mv, \tag{3.12}$$

$$\text{potential :} \quad k_0 \sim mv^2, \quad \vec{k} \sim mv, \tag{3.13}$$

$$\text{usoft :} \quad k_\mu \sim mv^2. \tag{3.14}$$

The same regions can also be considered for the photon with momentum $P - k$. These regions can be associated with the fields appearing in the effective Lagrangians, see e.g. ref. [6].

According to the threshold expansion prescription an integrand is expanded in each domain to a required accuracy and the resulting integral is computed in dimensional regularization. A detailed analysis of the full expressions in eqs. (3.1) and (3.2) is quite similar. To be definite let us consider the integral which enters in eq. (3.1)

$$J = \int dk \frac{e^2 \bar{u}_n \gamma_\alpha (l_1 - k) \gamma_\beta v_{\bar{n}}}{[(k - l_1)^2] [k^2] [(k - P)^2]} \frac{\epsilon_X^\nu}{4} \text{Tr} \left[\mathcal{P}_{1\mu\nu} \Gamma^{\alpha\beta\mu}(k) \right]. \tag{3.15}$$

Keeping the denominators of the heavy quark propagators in $\Gamma^{\alpha\beta\mu}$ unexpanded

$$(p_1 - k)^2 - m^2 = \left(\frac{1}{2}P + \Delta - k \right)^2 - m^2 = k^2 - P_0 k_0 + 2(\vec{k} \cdot \vec{\Delta}) - \vec{\Delta}^2 + \frac{1}{4}P_0^2 - m^2, \tag{3.16}$$

$$(p_2 - k)^2 - m^2 = \left(\frac{1}{2}P - \Delta - k \right)^2 - m^2 = k^2 - P_0 k_0 - 2(\vec{k} \cdot \vec{\Delta}) - \vec{\Delta}^2 + \frac{1}{4}P_0^2 - m^2, \tag{3.17}$$

where $P_0 \sim m$, $P_0^2/4 - m^2 \sim (mv)^2$, $\vec{\Delta} \sim mv$. In the hard region, the small scalar products with $\vec{\Delta}$ and the term $P_0^2/4 - m^2 \ll m^2$ can be neglected resulting in

$$\left[\left(\frac{1}{2}P \pm \Delta - k \right)^2 - m^2 \right]_h \simeq k^2 - (kP), \tag{3.18}$$

which appear in the expressions (3.6) and (3.7) (up to small regularization term $\vec{\Delta}^2$). From dimensional counting one immediately finds

$$J_h \sim \frac{\bar{u}_n \Gamma v_n}{m^3}, \tag{3.19}$$

where Γ denotes the Dirac structure. Computing the hard integral J_h in dimensional regularization one finds the IR poles $1/\varepsilon$. These singularities must cancel in the sum with other contribution.

Expanding the integrand (3.15) in the soft region (3.12) yields

$$J_s \simeq \int dk \frac{e^2 \bar{u}_n \gamma_\alpha \not{1} \gamma_\beta v_{\bar{n}}}{[-2(kl_1)][k^2][4m^2]} \frac{\epsilon_X^\nu}{4} \text{Tr} \left[\mathcal{P}_{1\mu\nu} \Gamma_s^{\alpha\beta\mu}(k) \right], \quad (3.20)$$

where $\Gamma_s^{\alpha\beta\mu}(k)$ is given by (3.5) with

$$\begin{aligned} [D_Q]_s &\sim \frac{1}{[-2(k\omega)]} \left\{ \gamma^\beta (\phi - 1) \gamma^\alpha + \gamma^\alpha (1 - \phi) \gamma^\beta \right\}, \\ [D'_Q]_s &\sim \frac{1}{2m} \frac{1}{[-(k\omega)]} \left\{ \gamma^\beta \gamma^\mu \gamma^\alpha + \gamma^\alpha \gamma^\mu \gamma^\beta \right\} + \frac{1}{2m} \frac{k^\mu}{[-(k\omega)]^2} \left\{ \gamma^\beta (\phi + 1) \gamma^\alpha - \gamma^\alpha (1 - \phi) \gamma^\beta \right\}. \end{aligned} \quad (3.21)$$

Calculating the trace and performing the contractions in the numerator results in

$$J_s \sim \frac{1}{m^3} \bar{u}_n \Gamma_1 v_{\bar{n}} \int dk \frac{1}{[k^2] [-(k\omega)]^2} \sim \frac{\bar{u}_n \Gamma_1 v_{\bar{n}}}{m^3}. \quad (3.22)$$

As the integral in (3.22) is scaleless it therefore vanishes in the dimensional regularization, i.e. $J_s = 0$.

In the potential region (3.13), the expansion of the heavy quark propagator reads

$$\left[\left(\frac{1}{2} P \pm \Delta - k \right)^2 - m^2 \right]_p \simeq P_0^2/4 - m^2 - P_0 k_0 - \left(\vec{k} \pm \vec{\Delta} \right)^2. \quad (3.23)$$

The computation of the corresponding integral then yields

$$J_p \simeq \frac{1}{m} \bar{u}_n \Gamma_1 v_{\bar{n}} \int dk \frac{1}{[-\vec{k}^2] \left[P_0^2/4 - m^2 - P_0 k_0 - \left(\vec{k} + \vec{\Delta} \right)^2 \right]^2} + \left(\vec{\Delta} \rightarrow -\vec{\Delta} \right) \sim \bar{u}_n \Gamma_1 v_{\bar{n}} \frac{v^{-1}}{m^3}. \quad (3.24)$$

However the poles in k_0 in the integrand of eq. (3.24) lie in the same imaginary half-plane and therefore the integral over k_0 vanishes. This observation is also true for the higher order contributions in v appearing from this domain. We can therefore conclude that the potential region cannot contribute in this case.

In the ultrasoft domain (3.14), the heavy quark propagators are expanded as

$$\left[\left(k - \frac{1}{2} P \pm \Delta \right)^2 - m^2 \right]_{us} \simeq P_0^2/4 - m^2 - P_0 k_0 - \vec{\Delta}^2. \quad (3.25)$$

Performing the expansion of the integrand one gets

$$J_{us} \sim \frac{1}{m} \bar{u}_n \Gamma_1 v_{\bar{n}} \int dk \frac{1}{[k^2] \left[P_0^2/4 - m^2 - P_0 k_0 - \vec{\Delta}^2 \right]^2} \sim \bar{u}_n \Gamma_1 v_{\bar{n}} \frac{1}{m^3}. \quad (3.26)$$

This integral has the same scaling behavior $\sim m^{-3}$ as the hard integral J_h in eq. (3.19). One can also see that the integral in eq. (3.26) is UV divergent. The similar analysis can also be carried out for the second photon with momentum $k - P$. Therefore we conclude that the exact integral must be given by sum

$$J = J_h + J_{us}, \quad (3.27)$$

where J_{us} denotes the contributions from the both ultrasoft domains. This conclusion can be checked by explicit calculations. A similar conclusion for the two-photon diagrams in figure 1 has also been obtained in ref. [11].

Guided by this consideration we suggest that the additional relevant domain is described by the ultrasoft region. In order to find the description of the appropriate operator in the effective theory one has to integrate out hard and soft photons and leptons. After that the description of QED sector includes only collinear leptons and ultrasoft photons. The integration of the soft photon with the lepton and quark must be described in the framework of the effective theory.

Within the above picture the factorization of the decay amplitudes can be described as a sum of two contributions

$$\begin{aligned} \mathcal{A}_J = & \bar{u}_n \Gamma_J v_{\bar{n}} C_{\gamma\gamma}^{(J)} i \langle \mathcal{O}({}^3P_0) \rangle \\ & + C_\gamma \langle e^+ e^- | \bar{\xi}_n(0) Y_n^\dagger(0) \gamma_\perp^\sigma Y_{\bar{n}}(0) \xi_{\bar{n}}(0) \mathcal{O}^\sigma({}^3S_1) | \chi_{cJ} \rangle. \end{aligned} \quad (3.28)$$

The first term on r.h.s. of this equation corresponds to the hard domain with the hard photons, $C_{\gamma\gamma}^{(J)}$ denotes the corresponding hard coefficient function.

The second term on r.h.s. of eq. (3.28) corresponds to the domain with the ultrasoft photon. The operator $\mathcal{O}^\sigma({}^3S_1)$ is defined in eq. (2.11). The outgoing collinear leptons are described by fields $\bar{\xi}_n$ and $\xi_{\bar{n}}$ which defined as

$$\bar{\xi}_n(x) = \bar{\psi}_c(x) \frac{\not{n} \not{\gamma}}{4}, \quad \xi_{\bar{n}} = \frac{\not{\bar{n}} \not{\gamma}}{4} \psi_c(x). \quad (3.29)$$

The photon Wilson lines Y_n^\dagger and $Y_{\bar{n}}$ describe the interaction of the ultrasoft longitudinal photons with the energetic lepton and antilepton and read

$$Y_n^\dagger(0) = \text{Pexp} \left\{ ie \int_0^\infty ds n \cdot B^{us}(sn) \right\}, \quad Y_{\bar{n}}(0) = \bar{\text{Pexp}} \left\{ -ie \int_0^\infty ds \bar{n} \cdot B^{us}(s\bar{n}) \right\}, \quad (3.30)$$

where B_μ^{us} denotes the ultrasoft photon field. The appearance of these Wilson lines is related with the fact that in a general gauge the tree level diagram with attachments of $n \cdot B^{us}$ photon to the collinear field $\bar{\xi}_n$ describing the outgoing lepton¹ are resummed to the P-ordered exponents

$$\bar{\psi}_c \left(1 - e \not{B}^{us} \frac{1}{i \not{D}} \right) \simeq \bar{\xi}_n \left(1 + e n \cdot B^{us} \frac{1}{i(n \cdot D)} \right) \simeq \bar{\xi}_n Y_n^\dagger. \quad (3.31)$$

¹We assume electrical charge is measured in proton units (positron is particle and electron is antiparticle) that allows to use the same notation for the covariant derivative and Wilson lines as in QCD.

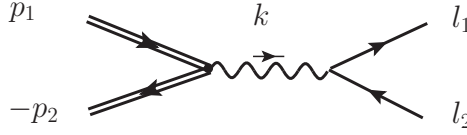


Figure 2. The hard one-photon exchange diagram.

The leading-order hard coefficient function C_γ is defined by the diagram in figure 2 and reads

$$C_\gamma = \frac{\alpha\pi}{m^2} eQ. \quad (3.32)$$

The soft and collinear modes in the effective action describing the QED sector are decoupled. This property is well known in the soft-collinear effective theory, see e.g. refs. [12–14]. This allows us to contract the lepton fields in the second matrix element in eq. (3.28) and rewrite it as

$$\langle e^+ e^- | \bar{\xi}_n(0) Y_n^\dagger(0) \gamma_\perp^\sigma Y_{\bar{n}}(0) \xi_{\bar{n}}(0) \mathcal{O}^\sigma(^3S_1) | \chi_{cJ} \rangle = \bar{u}_n \gamma_\perp^\sigma v_{\bar{n}} \langle 0 | \mathcal{O}_\gamma^\sigma(^3S_1) | \chi_{cJ} \rangle, \quad (3.33)$$

with

$$\mathcal{O}_\gamma^\sigma(^3S_1) \equiv Y_n^\dagger(0) Y_{\bar{n}}(0) \mathcal{O}^\sigma(^3S_1). \quad (3.34)$$

The presence of the soft scale $\bar{\Delta}^2$ in eqs. (3.9) and (3.10) can be explained by the contribution with ultrasoft photon. Therefore in order to find the hard coefficient functions $C_{\gamma\gamma}^{(J)}$ we have to perform the matching onto the configuration described by eq. (3.28). For that purpose we need to compute the ultrasoft matrix element (3.33) in the effective theory.

The interaction of ultrasoft photons with quarks are described within the pNRQED. The ultrasoft photons have momentum $p \sim mv^2$ so that photon field scales as

$$B_\mu^{us} \sim mv^2. \quad (3.35)$$

The scaling of the quark fields reads

$$\psi_\omega \sim (mv)^{3/2}, \quad \vec{\partial}_i \psi_\omega \sim (mv) \psi_\omega, \quad \partial_0 \psi_\omega \sim (mv^2) \psi_\omega. \quad (3.36)$$

Using this counting one finds

$$C_{\gamma\gamma}^{(J)} \mathcal{O}^\sigma(^3P_J) \sim m^{-3} (mv)^4. \quad (3.37)$$

At the same time

$$C_\gamma \mathcal{O}_\gamma^\sigma(^3S_1) \sim C_\gamma \mathcal{O}^\sigma(^3S_1) \sim m^{-2} (mv)^3. \quad (3.38)$$

However the pure quark operator $\mathcal{O}^\sigma(^3S_1)$ is C -odd and therefore it cannot contribute to the matrix element with a C -even charmonium state

$$\langle 0 | \mathcal{O}^\sigma(^3S_1) | \chi_{cJ} \rangle = 0. \quad (3.39)$$

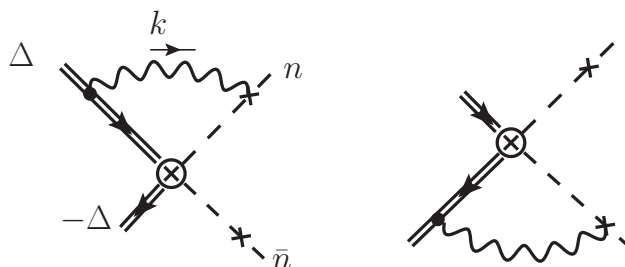


Figure 3. The diagrams generated by the T -product (3.43) in pNRQED. The crossed circle denotes the vertex of the operator $O_\gamma(^3S_1)$, the dashed lines represent the Wilson lines associated with light-like directions n and \bar{n} . The small crosses on the dashed lines show all possible attachments of the photon.

In order to obtain a nontrivial contribution one needs to consider at least one interaction of an ultrasoft photon with the quark in pNRQED. We only need the two-particle sector describing the electromagnetic interactions of quarks (in rest frame $\omega = (1, 0)$)

$$\mathcal{L}_0^{em}[B^{us}] = \int d^4x \psi_\omega^\dagger(x) \gamma_0 \left(i\omega \cdot \partial + \frac{i\partial_\top \cdot i\partial_\top}{2m} \right) \psi_\omega(x), \quad (3.40)$$

$$\mathcal{L}_1^{em}[B^{us}] = \int d^4x \psi_\omega^\dagger(x) \gamma_0 \left[\vec{x} \cdot \partial_\top ee_Q \omega \cdot B^{us}(x_0) + \frac{1}{m} ee_Q B^{us}(x_0) \cdot i\partial_\top \right] \psi_\omega(x), \quad (3.41)$$

and analogous contributions with antiquark fields. The arguments of the ultrasoft photon field are expanded because the space components of the quark fields varies at $\vec{x} \sim 1/mv$, the measure scales as $dx_0 \sim 1/mv^2$, $d^3\vec{x} \sim (mv)^{-3}$. With these rules one finds that $\mathcal{L}_0^{em} \sim v^0$ and $\mathcal{L}_1^{em} \sim v^1$. The leading-order term (3.40) provides the soft quark propagator

$$\Delta_\omega(k) = \frac{i}{(\omega k) - \vec{k}^2/2m + i\varepsilon}. \quad (3.42)$$

A nontrivial contribution to the matrix element $\langle 0 | \dots | \chi_{cJ} \rangle$ can be obtained from T -product

$$T\{\mathcal{O}_\gamma^\sigma(^3S_1), \mathcal{L}_1^{em}[B^{us}]\} \sim mv^4, \quad (3.43)$$

which is of the same order as the hard contribution in eq. (3.37). Calculation of this T -product gives diagrams shown in figure 3. The dashed lines can be associated with the collinear leptons or equivalently with the ultrasoft Wilson lines (3.30). These diagrams induce a mixing of the operators $O_\gamma^\sigma(^3S_1)$ and $\mathcal{O}(^3P_J)$ due to electromagnetic interaction in the framework of pNRQED.

In order to perform the matching onto operators according to formula (3.28) one has also to compute the contribution of the diagrams in figure 3. The simplest way to proceed is to follow the same technique as we used above for diagrams in figure 1.

Let us consider χ_{c2} as initial state. In this calculation we set $P_0 = 2m$ and only keep the relative momentum $\vec{\Delta}$. Then the sum of all four diagrams gives

$$\langle e^+ e^- | C_\gamma T\{\mathcal{O}_\gamma^\sigma(^3S_1), \mathcal{L}_1^{em}[B^{us}]\} | \chi_{c2} \rangle = \bar{u}_n \Gamma_2 v_{\bar{n}} i \langle \mathcal{O}(^3P_0) \rangle 4C_\gamma \frac{e^2 e_Q}{2m} J_{us}. \quad (3.44)$$

Computing these diagrams we project the soft quarks fields on the operator $\mathcal{O}({}^3P_2)$ and substitute the corresponding matrix element which gives the factor $\epsilon_\chi^{\sigma\rho} i \langle \mathcal{O}({}^3P_0) \rangle$, the coefficient 4 arises from the sum of the four diagrams shown in figure 3, the ultrasoft loop integral reads

$$J_{us} = (-i) \int dk \frac{1}{[k^2]} \frac{1}{[-(\omega k) - \vec{\Delta}^2/2m]^2}. \quad (3.45)$$

This integral coincides with the ultrasoft integral of eq. (3.26) obtained within the threshold expansion approach up to term $P_0^2/4 - m^2$ which vanishes because we set $P_0 = 2m$. The integral in eq. (3.45) is UV-divergent and we use dimension regularization $D = 4 - 2\epsilon$ in order to compute it. The result reads

$$J_{us} = \frac{\pi^{D/2}}{(2\pi)^D} \left(-\frac{2}{\epsilon}\right) \left(\frac{\vec{\Delta}^2}{m\mu_F}\right)^{-2\epsilon}, \quad (3.46)$$

where μ_F is the factorization scale. The $1/\epsilon$ pole is the UV-pole which describes UV-mixing of the operators $\mathcal{O}_\gamma^\sigma({}^3S_1)$ and $\mathcal{O}^\sigma({}^3P_J)$, schematically

$$[\mathcal{O}_\gamma({}^3S_1)]_R = \mathcal{O}_\gamma({}^3S_1) + Z_J \mathcal{O}({}^3P_J), \quad (3.47)$$

where $[\mathcal{O}]_R$ on the l.h.s. of eq. (3.47) denotes the renormalized operator. Furthermore, $Z_J \sim e^2/\epsilon$ is the corresponding renormalization constant. Assuming \overline{MS} -subtraction scheme one finds

$$[J_{us}]_R = \frac{1}{4\pi^2} \ln \frac{\vec{\Delta}^2}{m\mu_F}. \quad (3.48)$$

Hence we obtain

$$\langle e^+ e^- | C_\gamma T \{ \mathcal{O}_\gamma^\sigma({}^3S_1), \mathcal{L}_1^{em}[B^{us}] \} | \chi_{c2} \rangle_R = \bar{u}_n \Gamma_2 v_{\bar{n}} i \langle \mathcal{O}({}^3P_0) \rangle \frac{\alpha^2}{m^3} e_Q^2 2 \ln \frac{\vec{\Delta}^2}{m\mu_F}. \quad (3.49)$$

The soft matrix element for the χ_{c1} can be computed in the same way, resulting in

$$\langle e^+ e^- | C_\gamma T \{ \mathcal{O}_\gamma^\sigma({}^3S_1), \mathcal{L}_1^{em}[B^{us}] \} | \chi_{c1} \rangle_R = \bar{u}_n \Gamma_1 v_{\bar{n}} i \langle \mathcal{O}({}^3P_0) \rangle \frac{\alpha^2}{m^3} e_Q^2 2\sqrt{2} \ln \frac{m\mu_F}{\vec{\Delta}^2}. \quad (3.50)$$

The hard coefficients $C_{\gamma\gamma}^{(J)}$ are given by

$$C_{\gamma\gamma}^{(J)} = \frac{\mathcal{A}_J - C_\gamma \bar{u}_n \gamma_\perp^\sigma v_{\bar{n}} \langle 0 | \mathcal{O}_\gamma^\sigma({}^3S_1) | \chi_{cJ} \rangle}{\bar{u}_n \Gamma_J v_{\bar{n}} \langle 0 | \mathcal{O}^\sigma({}^3P_J) | \chi_{cJ} \rangle}, \quad (3.51)$$

where the expressions for \mathcal{A}_J are given by eqs. (3.9) and (3.10). The important check of the factorization formula (3.28) is the cancellation of the ultrasoft scale $\vec{\Delta}^2$ in the expressions for $C_{\gamma\gamma}^{(J)}$ obtained from eq. (3.51). Substituting the computed expressions in eq. (3.51) we obtain

$$C_{\gamma\gamma}^{(1)} = \frac{\alpha^2}{m^3} e_Q^2 \sqrt{2} \ln \frac{m^2}{4\mu_F^2}, \quad (3.52)$$

$$C_{\gamma\gamma}^{(2)} = \frac{\alpha^2}{m^3} e_Q^2 \left\{ \ln \frac{\mu_F^2}{m^2} + \frac{2}{3} (\ln 2 - 1 + i\pi) \right\}. \quad (3.53)$$

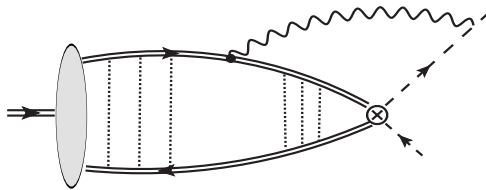


Figure 4. An example of the diagram in pNRQCD describing the ultrasoft matrix element of eq. (3.33). The dotted lines denote potential gluons with momenta given by eq. (3.13).

These expressions are the main result of this section. We observe that the soft scale cancel in eqs. (3.52) and (3.53) as it must be. Hence the factorization formula described by eq. (3.28) describes properly the ultrasoft region of the one-loop diagram.

The coefficient function $C_{\gamma\gamma}^{(2)}$ has an imaginary part which originates from the two-photon cut. Such mechanism can not work for χ_{c1} state, therefore $C_{\gamma\gamma}^{(1)}$ is real.

The hard coefficient functions depend on the factorization scale μ_F . Therefore

$$\mathcal{A}_J = \bar{u}_n \Gamma_J v_{\bar{n}} C_{\gamma\gamma}^{(J)}(\mu_F) i \langle \mathcal{O}({}^3P_0) \rangle + C_\gamma \bar{u}_n \gamma^\sigma v_{\bar{n}} \langle 0 | \mathcal{O}_\gamma^\sigma({}^3S_1) | \chi_{cJ} \rangle (\mu_F), \quad (3.54)$$

and the independence of the amplitude \mathcal{A}_J on μ_F yields the evolution equation

$$\bar{u}_n \Gamma_J v_{\bar{n}} i \langle \mathcal{O}({}^3P_0) \rangle \mu_F \frac{d}{d\mu_F} C_{\gamma\gamma}^{(J)}(\mu_F) = -C_\gamma \bar{u}_n \gamma^\sigma v_{\bar{n}} \mu_F \frac{d}{d\mu_F} \langle 0 | \mathcal{O}_\gamma^\sigma({}^3S_1) | \chi_{cJ} \rangle (\mu_F). \quad (3.55)$$

The solution of this equation depends on the initial condition defined at some scale μ_0 . Performing numerical estimates one has to fix a value of this scale. By derivation this scale separates the hard region (two hard photons) from the ultrasoft region (hard and ultrasoft photons). Therefore it is natural to associate this scale with the virtuality of the ultrasoft photon and to set μ_0 to be of order 300 – 500 MeV. Then the matrix element of the operator $\mathcal{O}_\gamma^\sigma({}^3S_1)$ on the r.h.s. of eq. (3.54) describes only the ultrasoft nonperturbative contribution which can be only estimated within some low-energy effective theory or model. Similar to the well known color octet mechanism, the operator $\mathcal{O}_\gamma^\sigma({}^3S_1)$ can also be associated with the electromagnetic mechanism. The corresponding matrix element can be interpreted as an overlap with the higher Fock state $|Q\bar{Q}\gamma\rangle$ which includes a dynamical photon while the matrix elements of the operators $\mathcal{O}({}^3P_J)$ describe the coupling to the dominant quark-antiquark state. Therefore the full description of the leptonic decay requires a knowledge on the subleading structure of the quarkonium state.

In the large mass limit $m \rightarrow \infty$ one can consider a specific situation known as the Coulomb limit when the binding energy is larger than the typical hadronic scale $E \sim mv^2 \gg \Lambda_{\text{QCD}}$. In this case the strong coupling is quite small $\alpha_s(mv) \sim v$ and ultrasoft contribution can be estimated within the pNRQCD. Then one has to compute the diagram as in figure 4 resumming the interactions with Coulomb gluons. Such calculation has been carried out for the radiation function in ref. [15]. Perhaps, such calculation might also be interesting here in order to get an idea about the relative value of this matrix element in the Coulomb limit. In present paper we will obtain an estimate of the ultrasoft matrix element using the so-called heavy hadron chiral perturbation theory (HH χ PT) framework in the next section.

4 Phenomenology

4.1 Calculation of the ultrasoft matrix element in the heavy hadron chiral perturbation theory

In order to provide a numerical estimate of the decay rate we need to estimate the ultrasoft matrix elements

$$\langle 0 | \mathcal{O}_\gamma^\sigma(^3S_1) | \chi_{cJ} \rangle \quad (4.1)$$

which describes an overlap with the higher Fock component of the charmonium state χ_{cJ} in which a dynamical photon is present. One can expect that the soft photon has already quite large wavelength and therefore it interacts with heavy charmonium as with a point-like source. Then it is natural to expect that the relevant dynamical degrees of freedom in this case are associated with mesonic fields and the corresponding low energy dynamics is described by the most generic effective action compatible with the symmetries of NRQCD. Such an approach is known as heavy hadron chiral perturbation theory in refs. [16, 17] for the heavy-light mesons and then generalized on quarkonia in refs. [18–20]. This framework can also be used for the calculation of the matrix element in eq. (4.1).

For our purpose we need only the electromagnetic sector of the HH χ PT described by the effective action which includes the kinetic terms for J/ψ and ψ' states and the vertices describing the electromagnetic vertices $\chi_{cJ} J/\psi \gamma$ and $\chi_{cJ} \psi' \gamma$.² As before we assume the rest frame for the initial state χ_{cJ} . The kinetic Lagrangian reads

$$\mathcal{L}_{\text{kin}}(x) = \frac{1}{2} 2M_\chi \psi_\mu^{(\omega)}(x) \{i(\omega\partial) - \Delta M\} \psi_\mu^{(\omega)}(x) + \frac{1}{2} 2M_\chi \psi'_\mu^{(\omega)}(x) \{i(\omega\partial) - \Delta' M\} \psi'_\mu^{(\omega)}(x), \quad (4.2)$$

with the residual masses $\Delta M = (M_\chi^2 - M_\psi^2)/2M_\chi$ and $\Delta' M = (M_\chi^2 - M_{\psi'}^2)/2M_\chi$. The fields $\psi_\mu^{(\omega)}$ and $\psi'_\mu^{(\omega)}$ describes the residual motion of the heavy J/ψ and ψ' particles and satisfy $\omega^\mu \psi_\mu^{(\omega)}(x) = \omega^\mu \psi'_\mu^{(\omega)}(x) = 0$.

The leading-order in $1/m$ effective Lagrangian describing the radiative decays $\chi_{cJ} \rightarrow J/\psi + \gamma$ and $\psi' \rightarrow \chi_{cJ} + \gamma$ reads [20]

$$\mathcal{L}_{SP}^{em} = \frac{1}{2} ee_Q f_\gamma \text{Tr} \left[\gamma_0 J_S^\dagger \gamma_0 J_P^\mu \right] F_{\mu\nu} \omega^\nu + \mathcal{L}_{SP}^{em} + \frac{1}{2} ee_Q f'_\gamma \text{Tr} \left[\gamma_0 J_S'^\dagger \gamma_0 J_P'^\mu \right] F_{\mu\nu} \omega^\nu + h.c. \quad (4.3)$$

with

$$J_S = \frac{1}{2}(1 + \phi) \left\{ \psi_\alpha^{(\omega)} \gamma^\alpha - \eta_c \gamma_5 \right\} \frac{1}{2}(1 - \phi), \quad (4.4)$$

$$J_S' = \frac{1}{2}(1 + \phi) \left\{ \psi'_\alpha^{(\omega)} \gamma^\alpha - \eta'_c \gamma_5 \right\} \frac{1}{2}(1 - \phi), \quad (4.5)$$

and

$$J_P^\mu = \frac{1}{2}(1 + \phi) \left\{ \chi_2^{\mu\alpha} \gamma_\alpha + \frac{1}{\sqrt{2}} i \varepsilon^{\mu\alpha\beta\rho} \gamma_\alpha \chi_{1\beta} \omega_\rho + \frac{1}{\sqrt{3}} (\gamma^\mu - \omega^\mu) \chi_0 + h_c^\mu \gamma_5 \right\} \frac{1}{2}(1 - \phi). \quad (4.6)$$

²We are grateful to Maxim Polyakov for discussion of the contribution with the virtual state ψ' .

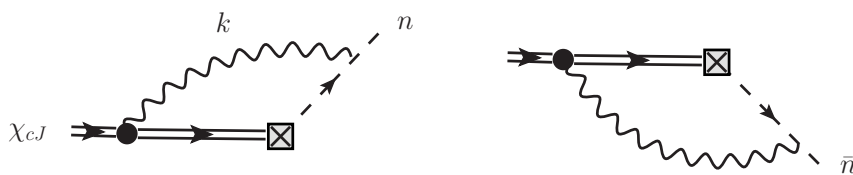


Figure 5. The diagrams which describe the matrix element (4.12) in $\text{HH}\chi\text{PT}$. The crossed box denotes the operator (4.11), dashes lines describe the Wilson lines Y_n^\dagger and $Y_{\bar{n}}$, black circle corresponds to the interaction vertices generated by \mathcal{L}_{SP}^{em} (4.3).

The currents J_S, J'_S and J_P^μ describe particles from S - and P -wave multiplets, respectively. In eq. (4.3) we introduced the dimensionless couplings f_γ and f'_γ . The fields χ_J describe charmonium states χ_{cJ} . Computing the trace in eq. (4.3) one finds

$$\mathcal{L}_{SP}^{em} = ee_Q f_\gamma \chi_2^{\mu\alpha} \psi_\alpha^{(\omega)} F_{\mu\nu} \omega^\nu + \frac{ee_Q f_\gamma}{\sqrt{2}} i\varepsilon^{\mu\alpha\beta\rho} \psi_\alpha^{(\omega)} \chi_{1\beta} \omega_\rho F_{\mu\nu} \omega^\nu \quad (4.7)$$

$$+ ee_Q f'_\gamma \chi_2^{\mu\alpha} \psi'_\alpha^{(\omega)} F_{\mu\nu} \omega^\nu + \frac{ee_Q f'_\gamma}{\sqrt{2}} i\varepsilon^{\mu\alpha\beta\rho} \psi'_\alpha^{(\omega)} \chi_{1\beta} \omega_\rho F_{\mu\nu} \omega^\nu + \dots \quad (4.8)$$

where we show only the relevant terms.

Our calculations involve operators $\mathcal{O}(^3P_J)$ and $\mathcal{O}(^3S_1)$ which have also to be matched onto physical quarkonium fields. The spin symmetry in the heavy quark limit yields

$$[\mathcal{O}^\sigma(^{2s+1}S_1)]_{\alpha\beta} = \langle \mathcal{O}(^3S_1) \rangle [J]_{\alpha\beta} + \langle \mathcal{O}'(^3S_1) \rangle [J']_{\alpha\beta}, \quad (4.9)$$

$$[\mathcal{O}^\mu(^{2s+1}P_J)]_{\alpha\beta} = \langle \mathcal{O}(^3P_0) \rangle [J^\mu]_{\alpha\beta}, \quad (4.10)$$

where $\alpha\beta$ are spinor indices. Taking the matrix element and computing the traces one can see that eqs. (4.9) and (4.10) reproduce correctly the matrix elements (2.16)–(2.20). Using these results one finds

$$\mathcal{O}_\gamma^\sigma(^3S_1) \simeq \left\{ \langle \mathcal{O}(^3S_1) \rangle \psi^{(\omega)\sigma}(0) + \langle \mathcal{O}'(^3S_1) \rangle \psi'^{(\omega)\sigma}(0) \right\} Y_n^\dagger Y_{\bar{n}}. \quad (4.11)$$

Hence

$$\langle 0 | \mathcal{O}_\gamma^\sigma(^3S_1) | \chi_{cJ} \rangle = \langle 0 | T \left\{ \left(\langle \mathcal{O}(^3S_1) \rangle \psi^{(\omega)\sigma}(0) + \langle \mathcal{O}'(^3S_1) \rangle \psi'^{(\omega)\sigma}(0) \right) Y_n^\dagger Y_{\bar{n}}, \mathcal{L}_{SP}^{em} \right\} | \chi_{cJ} \rangle. \quad (4.12)$$

Computing the T -product in eq. (4.12) gives the diagrams in figure 5. These diagrams are UV-divergent and we use in our calculation the dimensional regularization and \overline{MS} subtraction scheme. The results read

$$\langle 0 | \mathcal{O}_\gamma^\sigma(^3S_1) | \chi_{c1} \rangle = -i\varepsilon_\perp[\sigma\alpha] \epsilon_\chi^\alpha i \frac{\alpha}{\pi} e_Q \frac{1}{\sqrt{2}} h(\mu_\chi), \quad (4.13)$$

$$\langle 0 | \mathcal{O}_\gamma^\sigma(^3S_1) | \chi_{c2} \rangle = \epsilon_\chi^{\alpha\sigma} n_\alpha i \frac{\alpha}{\pi} e_Q h(\mu_\chi), \quad (4.14)$$

where $i\varepsilon_\perp[\sigma\alpha] \equiv i\varepsilon^{\sigma\alpha\beta\rho} n_\beta \bar{n}_\rho / 2$ and

$$h(\mu_\chi) = f_\gamma \langle \mathcal{O}(^3S_1) \rangle \frac{\Delta M}{M_\chi} \left(\ln 2 - 1 - \ln \frac{\mu_\chi}{\Delta M} - i\pi \right) + f'_\gamma \langle \mathcal{O}'(^3S_1) \rangle \frac{\Delta' M}{M_\chi} \left(\ln 2 - 1 - \ln \frac{\mu_\chi}{-\Delta' M} \right). \quad (4.15)$$

From these results one sees that the spin symmetry of NRQCD relates the soft photon matrix elements for $J = 1$ and $J = 2$ which are defined by the same nonperturbative couplings $f_\gamma \langle \mathcal{O}(^3S_1) \rangle$ and $f'_\gamma \langle \mathcal{O}'(^3S_1) \rangle$. The imaginary part in eq. (4.15) corresponds to the photon-quarkonium (J/ψ) cut in the diagrams in figure 5. Hence we conclude that the two-photon cut appears only in the hard photon contribution. The contribution with ψ' has no physical cut and in the diagram this is provided by the negative value of $\Delta'M$.

The UV-poles in the $\text{HH}\chi\text{PT}$ diagrams appear due to the mixing of the operators $\mathcal{O}_\gamma^\sigma(^3S_1)$ and χ_{cJ} . Therefore this UV-pole can be absorbed into renormalization of the chiral constant in front of the operators χ_{cJ} .³ The expression for the total amplitude now reads

$$\mathcal{A}_1 = i\bar{u}_n \Gamma_1 v_{\bar{n}} \left\{ \tilde{C}_1(\mu_\chi) + C_\gamma \frac{\alpha}{\pi} e_Q \frac{1}{\sqrt{2}} h(\mu_\chi) \right\}, \quad (4.16)$$

$$\mathcal{A}_2 = i\bar{u}_n \Gamma_2 v_{\bar{n}} \left\{ \tilde{C}_2(\mu_\chi) + C_\gamma \frac{\alpha}{\pi} e_Q h(\mu_\chi) \right\}. \quad (4.17)$$

We set the value of the chiral scale $\mu_\chi = \mu_0$, defining the chiral couplings $\tilde{C}_J(\mu_0)$ as product of the two-photon hard coefficient functions $C_{\gamma\gamma}^{(J)}$ and constant $\langle \mathcal{O}(^3P_0) \rangle$

$$\tilde{C}_J(\mu_0) = C_{\gamma\gamma}^{(J)}(\mu_0) \langle \mathcal{O}(^3P_0) \rangle. \quad (4.18)$$

This defines the expressions for the amplitudes which will be used for our numerical estimates.

4.2 Numerical estimates

In order to perform numerical estimates we need the values of the nonperturbative parameters $\langle \mathcal{O}(^3S_1) \rangle$, $\langle \mathcal{O}(^3P_0) \rangle$ and f_γ . Two of them are related to the values of quarkonium wave function at the origin, see eqs. (2.21) and (2.23). Their absolute values have been estimated in ref. [21] using different models for the potential. In our numerical calculations we use the values obtained for Buchmüller-Tye potential [23]

$$|R'_{21}(0)|^2 \simeq 0.075 \text{GeV}^5, \quad (4.19)$$

$$|R_{10}(0)|^2 \simeq 0.81 \text{GeV}^3, \quad |R_{20}(0)|^2 \simeq 0.530 \text{GeV}^3 \quad (4.20)$$

We also assume that they correspond to positive values:

$$R_{10}(0) > 0, \quad R_{20}(0) > 0, \quad R'_{21}(0) > 0. \quad (4.21)$$

The absolute values of the electromagnetic couplings f_γ and f'_γ can be estimated from the decays $\chi_{cJ} \rightarrow J/\psi\gamma$ and $\psi' \rightarrow \chi_{cJ}\gamma$. Using for widths $\Gamma[\chi_{c1}] = 0.84 \times 10^{-3} \text{GeV}$, $\Gamma[\chi_{c2}] = 1.93 \times 10^{-3} \text{GeV}$ and branching fractions $Br[\chi_{c1} \rightarrow J/\psi\gamma] = 0.340$, $Br[\chi_{c2} \rightarrow J/\psi\gamma] = 0.192$ from [22] we obtain

$$|f_\gamma| = \sqrt{\frac{\Gamma[\chi_{cJ}] Br[\chi_{cJ} \rightarrow J/\psi\gamma]}{\frac{1}{2} \alpha e_Q^2 k_0^3 / M_{\chi_{cJ}}^2}} \simeq \begin{cases} 5.87 (\chi_{c0}) \\ 6.05 (\chi_{c1}) \\ 6.03 (\chi_{c2}) \end{cases} \simeq 6.0, \quad (4.22)$$

³Or equivalently one can say that this pole renormalizes the contact vertex describing the $\chi_{cJ} \rightarrow e^+e^-$ decay.

| μ_0, MeV | $\Gamma[\chi_{c1} \rightarrow e^- e^+], \text{eV}$ | $\Gamma[\chi_{c2} \rightarrow e^- e^+], \text{eV}$ |
|---------------------|--|--|
| 300 | $0.060_s + 0.009_{hs} + 0.023_h = 0.091$ | $0.036_s + 0.020_{hs} + 0.016_h = 0.072$ |
| 400 | $0.063_s + 0.013_{hs} + 0.011_h = 0.087$ | $0.038_s + 0.017_{hs} + 0.013_h = 0.068$ |
| 500 | $0.066_s + 0.011_{hs} + 0.004_h = 0.082$ | $0.040_s + 0.015_{hs} + 0.010_h = 0.065$ |

Table 1. Numerical results for the decay widths for different values of the factorization scale μ_0 .

where $k_0 = (M_{\chi_{cJ}}^2 - M_\psi^2)/2M_{\chi_{cJ}}$ is the photon energy. Similarly, using widths $\Gamma[\psi'] = 0.299 \times 10^{-3} \text{GeV}$ and branching fractions $Br[\psi' \rightarrow \chi_{c1}\gamma] = 0.096$, $Br[\psi' \rightarrow \chi_{c2}\gamma] = 0.091$ from [22] we obtain

$$|f'_\gamma| = \left\{ \begin{array}{l} 6.5 (\chi_{c0}\gamma) \\ 7.0 (\chi_{c1}\gamma) \\ 8.1 (\chi_{c2}\gamma) \end{array} \right\} \simeq 7.2, \quad (4.23)$$

We also need to know the sign of this coupling which can only be defined by a specific nonperturbative calculation. It turns out that this coupling can be represented as an overlap integral of the radial wave functions. Comparing our results for the decay amplitudes $\chi_{cJ} \rightarrow J/\psi\gamma$ with the ones computed in ref. [24] we find

$$f_\gamma = \sqrt{2M_\chi} \sqrt{2M_\psi} \frac{1}{\sqrt{3}} \int_0^\infty dr r^3 R_{21}(r) R_{10}(r), \quad (4.24)$$

where factors $\sqrt{2M}$ appear due to relativistic normalizations of the hadronic states. The analogous expression also holds for the coupling f'_γ . The overlap integral has been computed in the framework of potential models, see e.g. refs. [25, 26]. Its value is found to be positive for f_γ and negative for f'_γ . Therefore we assume in the following that $f_\gamma > 0$ and $f'_\gamma < 0$.

The expressions for the decay width read

$$\Gamma[\chi_{cJ} \rightarrow e^+ e^-] = \left\{ \begin{array}{l} \frac{1}{12\pi} M_\chi |C_{\gamma\gamma}^{(1)}(\mu_0) \langle \mathcal{O}({}^3P_0) \rangle + C_\gamma \frac{\alpha}{\pi} e_Q h(\mu_0)/\sqrt{2} |^2 \\ \frac{1}{40\pi} M_\chi |C_{\gamma\gamma}^{(2)}(\mu_0) \langle \mathcal{O}({}^3P_0) \rangle + C_\gamma \frac{\alpha}{\pi} e_Q h(\mu_0) |^2 \end{array} \right., \quad (4.25)$$

where C_γ is given by eq. (3.32). We use $m_c = 1.5 \text{GeV}$ for the mass of the charm quark and compute $h(\mu_0)$ by substituting $M_\chi = (M_{\chi_{c1}} + M_{\chi_{c2}})/2$ in the expression (4.15).

Our numerical results are presented in table 1 for different values of μ_0 . The subscripts s and h denote contributions from the soft and hard photon terms and hs corresponds to the interference of these contributions. In all cases the largest numerical contribution is provided by the ultrasoft matrix element. This contribution is relatively large and it weakly depends on the factorization scale μ_0 . Our estimates for $\Gamma[\chi_{c1} \rightarrow e^- e^+]$ is approximately factor 5 smaller than the estimate in ref. [1] and in a good agreement with the estimate in ref. [2]. For $\Gamma[\chi_{c2} \rightarrow e^- e^+]$ our result is five times larger than one obtained in ref. [1].

From table 1 one can observe that the interference of the hard and ultrasoft contributions is numerically large for χ_{c2} width and relatively small for χ_{c1} . This can be explained as following. The imaginary part of $h(\mu_0)$ is numerically much larger than the real one, see eq. (4.15). Further, the hard coefficient function $C_{\gamma\gamma}^{(1)}$ is real and therefore corresponding interference in the width depends only from the real part of $h(\mu_0)$. The imaginary part of

$C_{\gamma\gamma}^{(2)}$ is not zero and therefore in this case the interference depends on the large imaginary part $h(\mu_0)$ and turns out numerically large. This observation allows one to conclude that the decay width χ_{c2} is quite sensitive to the relative sign of parameters R_{10} and R'_{21} . In our estimate we used that these parameters has the same sign, see eq. (4.21). However if they have opposite sign then the interference contribution is negative and this reduces the numerical value of the $\Gamma[\chi_{c2} \rightarrow e^-e^+]$ by factor 2.

In ref. [1] it was shown that unitarity and analyticity allows one to constrain the minimal values of decay widths

$$\Gamma[\chi_{c1} \rightarrow e^-e^+] \geq \frac{3}{2} \frac{\alpha}{k_0} \Gamma[J/\psi \rightarrow e^-e^+] \Gamma[\chi_{c1} \rightarrow \gamma J/\psi] \approx 0.046 \text{ eV}, \quad (4.26)$$

$$\Gamma[\chi_{c2} \rightarrow e^-e^+] \geq \left(\sqrt{\frac{\alpha^2}{9} \Gamma[\chi_{c2} \rightarrow \gamma\gamma]} + \sqrt{\frac{9\alpha^2}{20k_0} \Gamma[\chi_{c2} \rightarrow \gamma J/\psi] \Gamma[J/\psi \rightarrow e^-e^+]} \right)^2 \approx 0.037 \text{ eV}. \quad (4.27)$$

In the presented formalism these constrains are always satisfied because the soft contribution has a cut which yields the imaginary part required for the saturation of the bounds in eqs. (4.26) and (4.27). Therefore all our estimates shown in table I are in agreement with these inequalities. As one can see from table I the hard two-photon contribution is always smaller than the limiting value in both cases. The same observation was also made in ref. [1]. This clearly indicates that the soft photon configuration provides a critically important contribution to these decay amplitudes.

The derived approach can also be used for a description of leptonic decays of bottomonium states χ_{bJ} . These particles have almost the same branching fractions for $\chi_{bJ} \rightarrow \Upsilon(1S)\gamma$ decay, see e.g. [22], but at present the widths of these states are not yet measured. Therefore, we cannot extract the decay coupling $f_\gamma^{(b)}$ using experimental data. Instead, we use the estimates for the corresponding widths obtained in the model with a Cornell potential [25]. The corresponding values can be found in ref. [26] and read

$$\Gamma[\chi_{b1}] = 27.8 \text{ keV}, \quad \Gamma[\chi_{b2}] = 31.6 \text{ keV}. \quad (4.28)$$

This gives for the dimensionless coupling in the HH χ PT Lagrangian

$$f_\gamma^{(b)} \simeq 9.4. \quad (4.29)$$

On the other hand, the width of $\Upsilon(2S)$ and branching fractions $\Upsilon(2S) \rightarrow \chi_{bJ}\gamma$ are known [22]:

$$\Gamma[\Upsilon(2S)] = 32 \text{ keV}, \quad Br[\Upsilon(2S)] \rightarrow \chi_{b1}\gamma = 0.06, \quad Br[\Upsilon(2S)] \rightarrow \chi_{b2}\gamma = 0.07. \quad (4.30)$$

Using this values we obtain

$$f_\gamma^{\prime(b)} \simeq -16. \quad (4.31)$$

The sign of the couplings $f_\gamma^{(b)}$ and $f_\gamma^{\prime(b)}$ in eqs. (4.29) and (4.31) is again defined with the help of the overlap representation as in eq. (4.24) and corresponding estimates given in ref. [26]. The corresponding radial wave functions at the origin read [21]

$$|R'_{21}(0)|^2 \simeq 2.067 \text{ GeV}^5, \tag{4.32}$$

$$|R_{10}(0)|^2 \simeq 14.05 \text{ GeV}^3, \quad |R_{20}(0)|^2 \simeq 5.7 \text{ GeV}^3. \tag{4.33}$$

With these values and taking $\mu_0 = 400\text{MeV}$ we obtain

$$\Gamma[\chi_{b1} \rightarrow e^- e^+] = (2.0_s + 0.9_{hs} + 1.1_h) \times 10^{-3} \simeq 4.0 \times 10^{-3} \text{ eV}, \tag{4.34}$$

$$\Gamma[\chi_{b2} \rightarrow e^- e^+] = (1.2_s + 0.15_{hs} + 0.4_h) \times 10^{-3} \simeq 1.7 \times 10^{-3} \text{ eV}. \tag{4.35}$$

We observe that in this case the contribution of the ultrasoft configuration also remains larger than the hard one.

5 Conclusions

The decay width $\Gamma[\chi_{cJ} \rightarrow e^- e^+]$ was computed using a factorization NRQCD approach. The dominant partonic subprocess was described by the annihilation of the heavy quark-antiquark pair into two photons: $c\bar{c} \rightarrow \gamma^* \gamma^* \rightarrow e^+ e^-$. The corresponding contribution is given by the one-loop diagram with two photons in the intermediate state. The dominant regions in the loop integral are associated with two configurations: hard photons and one ultrasoft and hard photons. The soft part of the contribution with ultrasoft photon overlaps with the higher Fock state $|Q\bar{Q}\gamma\rangle$ of the heavy meson, while the hard contribution overlaps with the leading two quark state. We have demonstrated that these contributions can be factorized and described by two different operators in NRQCD effective theory. The ultrasoft photon contribution is estimated using framework of the heavy hadron chiral perturbation theory. This allows us to obtain numerical estimates using a minimal set of the known nonperturbative parameters. Our estimates for charmonia χ_{c1} and χ_{c2} show that the ultrasoft photon configurations provide the numerically dominant contribution. This explains why the obtained numerical results for $\Gamma[\chi_{c1} \rightarrow e^- e^+]$ are in good agreement with the estimates obtained in ref. [2] where only the usoft contribution was considered. We also expect that the developed formalism can be helpful to perform a more systemic analysis of decays if charmonium-like state such as $X(3872) \rightarrow e^- e^+$.

Acknowledgments

We are grateful to Achim Denig for useful discussions. This work is supported by the Helmholtz Institute Mainz.

Open Access. This article is distributed under the terms of the Creative Commons Attribution License ([CC-BY 4.0](https://creativecommons.org/licenses/by/4.0/)), which permits any use, distribution and reproduction in any medium, provided the original author(s) and source are credited.

References

- [1] J.H. Kühn, J. Kaplan and E.G.O. Safiani, *Electromagnetic Annihilation of e^+e^- Into Quarkonium States with Even Charge Conjugation*, *Nucl. Phys. B* **157** (1979) 125 [INSPIRE].
- [2] A. Denig, F.-K. Guo, C. Hanhart and A.V. Nefediev, *Direct $X(3872)$ production in e^+e^- collisions*, *Phys. Lett. B* **736** (2014) 221 [arXiv:1405.3404] [INSPIRE].
- [3] G.P. Lepage, L. Magnea, C. Nakhleh, U. Magnea and K. Hornbostel, *Improved nonrelativistic QCD for heavy quark physics*, *Phys. Rev. D* **46** (1992) 4052 [hep-lat/9205007] [INSPIRE].
- [4] G.T. Bodwin, E. Braaten and G.P. Lepage, *Rigorous QCD analysis of inclusive annihilation and production of heavy quarkonium*, *Phys. Rev. D* **51** (1995) 1125 [Erratum *ibid.* **D 55** (1997) 5853] [hep-ph/9407339] [INSPIRE].
- [5] M. Beneke and V.A. Smirnov, *Asymptotic expansion of Feynman integrals near threshold*, *Nucl. Phys. B* **522** (1998) 321 [hep-ph/9711391] [INSPIRE].
- [6] N. Brambilla, A. Pineda, J. Soto and A. Vairo, *Effective field theories for heavy quarkonium*, *Rev. Mod. Phys.* **77** (2005) 1423 [hep-ph/0410047] [INSPIRE].
- [7] A. Pineda and J. Soto, *Effective field theory for ultrasoft momenta in NRQCD and NRQED*, *Nucl. Phys. Proc. Suppl.* **64** (1998) 428 [hep-ph/9707481] [INSPIRE].
- [8] A. Pineda and J. Soto, *The Lamb shift in dimensional regularization*, *Phys. Lett. B* **420** (1998) 391 [hep-ph/9711292] [INSPIRE].
- [9] N. Brambilla, A. Pineda, J. Soto and A. Vairo, *The Infrared behavior of the static potential in perturbative QCD*, *Phys. Rev. D* **60** (1999) 091502 [hep-ph/9903355] [INSPIRE].
- [10] N. Brambilla, A. Pineda, J. Soto and A. Vairo, *Potential NRQCD: An Effective theory for heavy quarkonium*, *Nucl. Phys. B* **566** (2000) 275 [hep-ph/9907240] [INSPIRE].
- [11] D. Yang and S. Zhao, $\chi_{QJ} \rightarrow l^+l^-$ within and beyond the Standard Model, *Eur. Phys. J. C* **72** (2012) 1996 [arXiv:1203.3389] [INSPIRE].
- [12] C.W. Bauer, S. Fleming, D. Pirjol, I.Z. Rothstein and I.W. Stewart, *Hard scattering factorization from effective field theory*, *Phys. Rev. D* **66** (2002) 014017 [hep-ph/0202088] [INSPIRE].
- [13] R.J. Hill and M. Neubert, *Spectator interactions in soft collinear effective theory*, *Nucl. Phys. B* **657** (2003) 229 [hep-ph/0211018] [INSPIRE].
- [14] M. Beneke and T. Feldmann, *Factorization of heavy to light form-factors in soft collinear effective theory*, *Nucl. Phys. B* **685** (2004) 249 [hep-ph/0311335] [INSPIRE].
- [15] M. Beneke, G.A. Schuler and S. Wolf, *Quarkonium momentum distributions in photoproduction and B decay*, *Phys. Rev. D* **62** (2000) 034004 [hep-ph/0001062] [INSPIRE].
- [16] M.B. Wise, *Chiral perturbation theory for hadrons containing a heavy quark*, *Phys. Rev. D* **45** (1992) 2188 [INSPIRE].
- [17] G. Burdman and J.F. Donoghue, *Union of chiral and heavy quark symmetries*, *Phys. Lett. B* **280** (1992) 287 [INSPIRE].
- [18] R. Casalbuoni, A. Deandrea, N. Di Bartolomeo, R. Gatto, F. Feruglio and G. Nardulli, *Effective Lagrangian for quarkonia and light mesons in a soft-exchange-approximation*, *Phys. Lett. B* **302** (1993) 95 [INSPIRE].

- [19] T. Mannel and G.A. Schuler, *Heavy quarkonium effective theory*, *Z. Phys. C* **67** (1995) 159 [[hep-ph/9410333](#)] [[INSPIRE](#)].
- [20] R. Casalbuoni, A. Deandrea, N. Di Bartolomeo, R. Gatto, F. Feruglio and G. Nardulli, *Phenomenology of heavy meson chiral Lagrangians*, *Phys. Rept.* **281** (1997) 145 [[hep-ph/9605342](#)] [[INSPIRE](#)].
- [21] E.J. Eichten and C. Quigg, *Quarkonium wave functions at the origin*, *Phys. Rev. D* **52** (1995) 1726 [[hep-ph/9503356](#)] [[INSPIRE](#)].
- [22] PARTICLE DATA GROUP collaboration, K.A. Olive et al., *Review of Particle Physics*, *Chin. Phys. C* **38** (2014) 090001 [[INSPIRE](#)].
- [23] W. Buchmüller and S.H.H. Tye, *Quarkonia and Quantum Chromodynamics*, *Phys. Rev. D* **24** (1981) 132 [[INSPIRE](#)].
- [24] N. Brambilla, P. Pietrulewicz and A. Vairo, *Model-independent Study of Electric Dipole Transitions in Quarkonium*, *Phys. Rev. D* **85** (2012) 094005 [[arXiv:1203.3020](#)] [[INSPIRE](#)].
- [25] E. Eichten, K. Gottfried, T. Kinoshita, K.D. Lane and T.-M. Yan, *Charmonium: The Model*, *Phys. Rev. D* **17** (1978) 3090 [*Erratum ibid.* **D 21** (1980) 313] [[INSPIRE](#)].
- [26] QUARKONIUM WORKING GROUP collaboration, N. Brambilla et al., *Heavy quarkonium physics*, [hep-ph/0412158](#) [[INSPIRE](#)].